

Low-temperature magnetic structure of YBaCuFeO₅ and the effect of partial substitution of yttrium by calcium

M. J. Ruiz-Aragón and E. Morán

Departamento de Química Inorgánica, Facultad de Ciencias Químicas, Universidad Complutense, E-28040, Madrid, Spain

U. Amador

Departamento de Química Inorgánica y Materiales, Facultad de Ciencias Experimentales y Técnicas, Universidad San Pablo-CEU, Urb. Montepríncipe, Boadilla del Monte, E-28668, Madrid, Spain

J. L. Martínez

Instituto de Ciencias de Materiales de Madrid, C.S.I.C., Cantoblanco, E-28049, Madrid, Spain

N. H. Andersen

Condensed Matter Physics and Chemistry Department, Risø National Laboratory, DK-4000 Roskilde, Denmark

H. Ehrenberg*

Materials Science, Darmstadt University of Technology, Petersenstrasse 23, D-64287 Darmstadt, Germany and Interdisciplinary Research Centre in Superconductivity, Madingley Road, Cambridge CB3 0HE, United Kingdom

(Received 25 August 1997; revised manuscript received 18 November 1997)

Two magnetic phase transitions at $T_{N1} \approx 475$ K (AF1 phase) and $T_{N2} \approx 240$ K (AF2) are observed in YBaCuFeO₅. The magnetic unit cell of AF1 is four times the chemical cell, $a_m = \sqrt{2}a$, $c_m = 2c$, and the magnetic moments within one chemical cell are antiparallel to each other. The magnetic unit cell of the low-temperature phase AF2 is similar to that of AF1 with $a_M = a_m$, but with a four times larger c_M axis, i.e., $c_M = 4c_m = 8c$ and a more complicated sequence along [001] than in AF1. Denoting the magnetic unit cell of AF1 as A, the magnetic unit cell of AF2 can be considered as built up from the sequence AA-A-A along [001]. In the Ca-doped compound, oxygen vacancies have a detrimental effect on the long-range correlation along [001]. As a consequence, two magnetic phases coexist: One phase with magnetic unit cell $a_1 = \sqrt{2}a$ and $c_1 = c$ appears at room temperature, and the Néel temperature, T_{N1} , for the other, predominant phase decreases as compared to the undoped compound. The transition to AF2 seems to be hindered, and AF1 is observed down to 8 K in (Y_{0.94}Ca_{0.06})BaCuFeO_{4.95}. [S0163-1829(98)06633-8]

INTRODUCTION

The title compound, YBaCuFeO₅, was prepared by Er-Rakho *et al.*¹ The structure of this material is closely related to that of YBa₂Cu₃O₇ and can be described as an oxygen-deficient twofold perovskite (ABO₃) superstructure. It consists of double layers of square pyramids (BO₅) sharing the apical oxygen, where Ba²⁺ ions occupy the perovskite cuboctahedral A position, and Y³⁺ cations are located between the layers. Regarding the B positions, there is some controversy in the literature. The results obtained by Er-Rakho *et al.*¹ from Mössbauer spectroscopy, suggested that iron ions are located in two nonequivalent positions. Therefore, based on their neutron powder-diffraction data, these authors have refined a structural model of $P4mm$ symmetry, in which two symmetry unrelated mixed-metal BO₂ layers with composition 0.62 Cu+0.38 Fe and 0.38 Cu+0.62 Fe, respectively, have been considered. However, based on the Mössbauer study by Meyer *et al.*,² Pissas *et al.*,^{3,4} claimed that copper and iron cations are located in separated layers. Furthermore, Mombro *et al.*⁵ refined the nuclear and magnetic structures of YBaCuFeO₅ in the noncentrosymmetric space group $P4mm$, this choice was made on the basis of the

works by Pissas *et al.*^{3,4} and on spectroscopic studies (Raman and IR) by Atanassova *et al.*⁶ that supported the acentric character of the structure. They found that the iron moments were perpendicular to the c axis and AF ordered within a layer, and no magnetic ordering was observed in the copper sublattice for the studied temperature range (300–500 K). The crystal structure of this phase has also been determined by single crystal x-ray diffraction,⁷ and the results support the use of the $P4mm$ space group.

Recently, Caignaert *et al.*⁸ and ourselves⁹ have studied the title compound by neutron powder diffraction. In both cases, the model for the nuclear structure was developed using the centrosymmetric space group $P4/mmm$, with iron and copper ions randomly distributed onto equivalent BO₂ layers. In Ref. 8 two magnetic phase transitions are reported at $T_{N1} = 441(2)$ K and $T_{N2} \approx 230$ K. The magnetic structure between T_{N1} and T_{N2} is described with a unit cell related to the crystallographic one by $a_m = \sqrt{2}a$ and $c_m = 2c$, the magnetic moments being tilted with respect to the c axis. These authors propose an incommensurate magnetic structure with a short-range order below T_{N2} . The intensity of the magnetic reflections ($h/2, k/2, l/2$) decreases on cooling, while both the magnetic satellites on each side of the magnetic peaks and the very weak peaks indexed as ($h/2, k/2, l$) increase. A

TABLE I. Structural parameters for YBaCuFeO₅ (YBCF) and (Y_{0.94}Ca_{0.06})BaCuFeO_{4.95} (YCa) at room temperature (298 K). YBaCuFeO₅: S.G: *P4/mmm*, $a=3.8740(2)$ Å, $c=7.6676(5)$ Å, $V=115.1(1)$ Å³, $R_p=0.073$, $R_{wp}=0.096$, $R_{Mag}=0.274$, $\chi^2=4.13$. (Y_{0.94}Ca_{0.06})BaCuFeO_{4.95}: S.G: *P4/mmm*, $a=3.8709(2)$ Å, $c=7.6656(4)$ Å, $V=114.8(1)$ Å³, $R_p=0.071$, $R_{wp}=0.103$, $R_B=0.047$, $R_{Mag1}=0.115$, $R_{Mag2}=0.22$, $\chi^2=6.27$.

Atom		Site	x/a	y/b	z/c		Occupation		$Beq/\text{Å}^2$	
YBCF	YCA				YBCF	YCa	YBCF	YCa	YBCF	YCa
	Ba	1a	0	0	0	0		1	0.9(1)	0.96(8)
Y	Y/Ca	1b	0	0	$\frac{1}{2}$	$\frac{1}{2}$	1	0.94/0.06	0.33(1)	0.63(6)
	CuFe	2h	$\frac{1}{2}$	$\frac{1}{2}$	0.2680(3)	0.2682(3)		1/1	0.47(4)	0.68(5)
	O(1)	4i	$\frac{1}{2}$	0	0.3156(2)	0.3146(2)	4	3.96(4)	0.85(5)	0.83(6)
	O(2)	1c	$\frac{1}{2}$	$\frac{1}{2}$	0	0		1	1.1(1)	1.5(1)

somewhat similar behavior is reported on tetragonal samples of YBa₂Cu₃O_{6+y} (YBCO) with $y < 0.35$ doped with Al (Refs. 10 and 11) and in Fe- and Co-doped YBCO for low doping levels.^{12,13} In these doped compounds a transition is observed from the high-temperature magnetic phase AF1, with spin ordering along the c axis $[+0-]$ and $c_m = c$, to the phase AFII, with sequences $[+0+]$ $[-0-]$, $[+-+]$ $[-+-]$ or $[+++]$ $[- - -]$ and $c_m = 2c$. However, components of both the AF1 and the AFII ordering sequences are observed over a very broad temperature range. Consistent with theoretical model analysis, the coexistence of the two ordering components has been interpreted as resulting from specific intermediate *turn angle* phases, TAI, TAI1, and TAI11.^{11,14} For higher levels of Fe and Co doping, the AFII phase is stabilized in the whole temperature range.

However, the structure of the analogous material YBaCo_{2-x}Cu_xO_{5+δ} ($0.3 \leq x \leq 1$) has been refined from neutron powder-diffraction data by Barbey *et al.*¹⁵ and Huang *et al.*¹⁶ in the space group *P4/mmm*. The magnetic structure of these compounds changes gradually with the cobalt/copper ratio: the magnetic moments are aligned parallel to the c axis for $x=1$ with a propagation vector $\mathbf{k} = (\frac{1}{2}, \frac{1}{2}, \frac{1}{2})$, while they lie on the basal plane for $x < 0.75$ with $\mathbf{k} = (\frac{1}{2}, \frac{1}{2}, 1)$; for intermediate values two magnetic transitions are found. When half of the copper atoms are replaced by iron in YBaCuCoO₅ (Ref. 17) the magnetic cell changes, the magnetic structure being similar to that observed in YBaCo_{2-x}Cu_xO_{5+δ} ($x < 0.7$).¹⁵

The magnetic behavior of PrBaCuFeO_{5+δ} is more complex. For samples with $\delta > 0$, no long-range magnetic order is observed,^{9,18} while the structure of the stoichiometric material can be described with two propagation vectors $\mathbf{k}_1 = (\frac{1}{2}, \frac{1}{2}, \frac{1}{2})$ and $\mathbf{k}_2 = (\frac{1}{2}, \frac{1}{2}, 1)$. Two equivalent models are possible: an incoherent mixture of domains of different phases and a canted structure.

Therefore, the magnetic behavior of LnBaCuMO₅ (Ln=lanthanide, $M=Fe, Co$) is an interesting and topical field of research. In this paper the magnetic structure of YBaCuFeO₅ below T_{N2} is presented and compared to the intermediate magnetic structure observed at room temperature. The effect of the partial substitution of yttrium by calcium on the magnetic properties is also reported.

EXPERIMENT

Samples have been prepared by the ‘‘nitrates method’’¹⁹ and were checked to be single phase by x-ray diffraction on a Siemens D-5000 diffractometer using monochromatic Cu($K\alpha$) radiation. Neutron diffraction was performed at different temperatures on the multidetector powder diffractometer at the DR3 reactor at Risø National Laboratory. A vanadium can of 9 mm diameter and 5 cm length was used as the sample container. Neutrons of wavelength 1.475(1) Å were chosen. Diffraction data were analyzed using the software packages FULLPROF²⁰ and GSAS.²¹

Thermogravimetric analysis was done in pure argon up to 1173 K using a Perkin-Elmer 3600 apparatus with a heating rate of 10°/min. Magnetic susceptibility was measured on a Lakeshore 7225 ac susceptometer/dc Magnetometer System working at different magnetic fields up to 5 T. The temperature range for the magnetic measurements spans from 1.7 to 800 K. The field dependence of magnetization was studied up to 12 T using a vibrating sample magnetometer from Oxford Instruments.

RESULTS AND DISCUSSION

Remarks on the nuclear structure

The best agreement between our neutron-diffraction data and calculated patterns were obtained for the structural model developed by Huang *et al.*¹⁶ for YBaCuFeO₅ in the space group *P4/mmm*. In this model iron and copper ions occupy one crystallographic position, being randomly distributed among the two equivalent BO₂ layers. We note that convergent beam electron diffraction on the same YBaCuFeO₅ sample used in the present studies gave strong evidence for a centrosymmetric structure, supporting the use of space group *P4/mmm*.²² Including the splitting of the Cu/Fe position, as proposed by Caignaert *et al.*,⁸ did not improve the reliability factors significantly. The structural parameters for YBaCuFeO₅ and (Y_{1-x}Ca_x)BaCuFeO_{5-δ} at room temperature are summarized in Table I, the corresponding observed and calculated patterns are shown in Figs. 1 and 2. The oxygen vacancies in the nonstoichiometric compound, $\delta=0.05(2)$, are situated on the O(1) site, i.e., in the basal plane of the square pyramids. As a consequence, some iron or copper ions are coordinated to four oxygens in

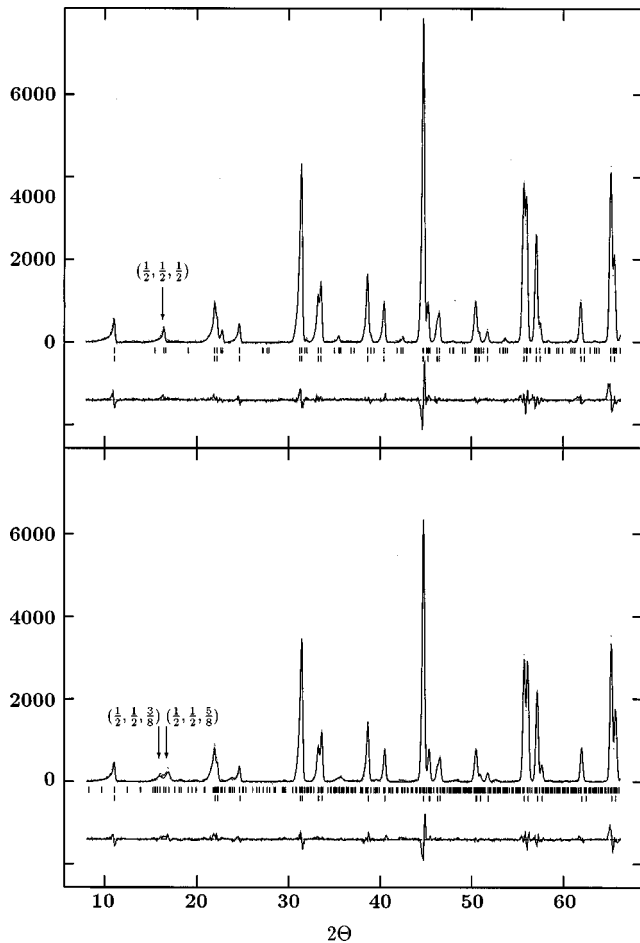


FIG. 1. Observed and calculated neutron-diffraction patterns at room temperature (top) and 8 K (bottom) for YBaCuFeO_5 ($\lambda = 1.475 \text{ \AA}$). The nuclear structure has space group $P4/mmm$, the magnetic structures correspond to the AF1 (room temperature) and AF2 (8 K) models.

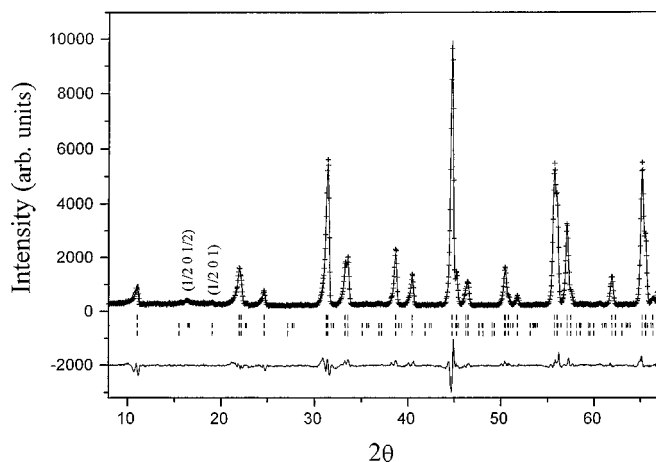


FIG. 2. Experimental and calculated neutron-diffraction patterns at room temperature for $(\text{Y}_{0.94}\text{Ca}_{0.06})\text{BaCuFeO}_{4.95}$. The models of both the nuclear structure and the structure of the major magnetic phase are similar to those used in the undoped material. Poorly defined peaks belong to a secondary magnetic phase with unit cell $a_m = \sqrt{2}a$ and $c_m = c$.

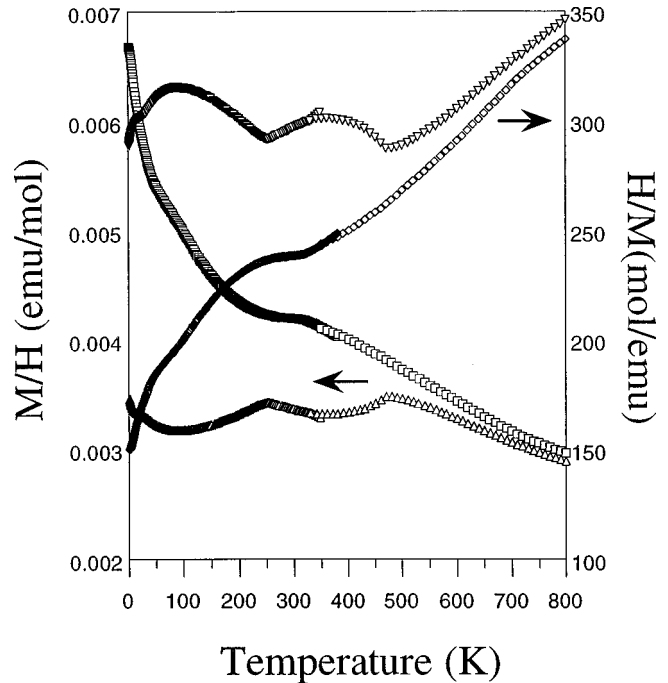


FIG. 3. Molar susceptibility and inverse molar susceptibility vs temperature for YBaCuFeO_5 (up and down triangles, respectively) and for $\text{Y}_{0.94}\text{Ca}_{0.06}\text{BaCuFeO}_{4.95}$ (squares and rhombuses, respectively).

a very distorted tetrahedral environment. The actual Y/Ca ratio of this sample was determined from x-ray powder diffraction because of the better contrast of these elements for x rays than for neutrons. Combining both techniques results in the composition $(\text{Y}_{0.94(2)}\text{Ca}_{0.06(2)})\text{BaCuFeO}_{4.95(2)}$.

MAGNETIC STRUCTURE

Magnetic behavior

As deduced from the magnetic susceptibility measurements and Mössbauer spectroscopy, the compounds LnBaCuFeO_5 (Ln=lanthanide) are antiferromagnetically ordered at room temperature,^{1-3,8,19} and the Néel temperature T_N is about 460 K for YBaCuFeO_5 .¹ The magnetic ordering is strongly affected by the replacement of yttrium by other rare-earth elements like praseodymium,^{3,9,18} the presence of extra oxygen in the structure,^{3,4,9,18} or even by low levels of doping on the yttrium site, as will be shown.

Figure 3 shows the molar magnetic susceptibility and the inverse susceptibility versus temperature for YBaCuFeO_5 . A first antiferromagnetic transition is observed at $T_{N1} \approx 475 \text{ K}$ and a second well-defined transition is found at $T_{N2} \approx 240 \text{ K}$. At low temperatures ($T \approx 20 \text{ K}$) a third anomaly is observed.

The field dependence (up to 12 T) of magnetization in YBaCuFeO_5 is shown in Fig. 4. The data for 8 and 250 K have been fitted by a linear dependence, while those corresponding to 150 and 200 K are described by a field-induced transition between two phases with a linear $M(H)$ relation for each phase:

$$M(H) = 1/2\{M_1[1 - \tanh(H - H_C)/\sigma]\}$$

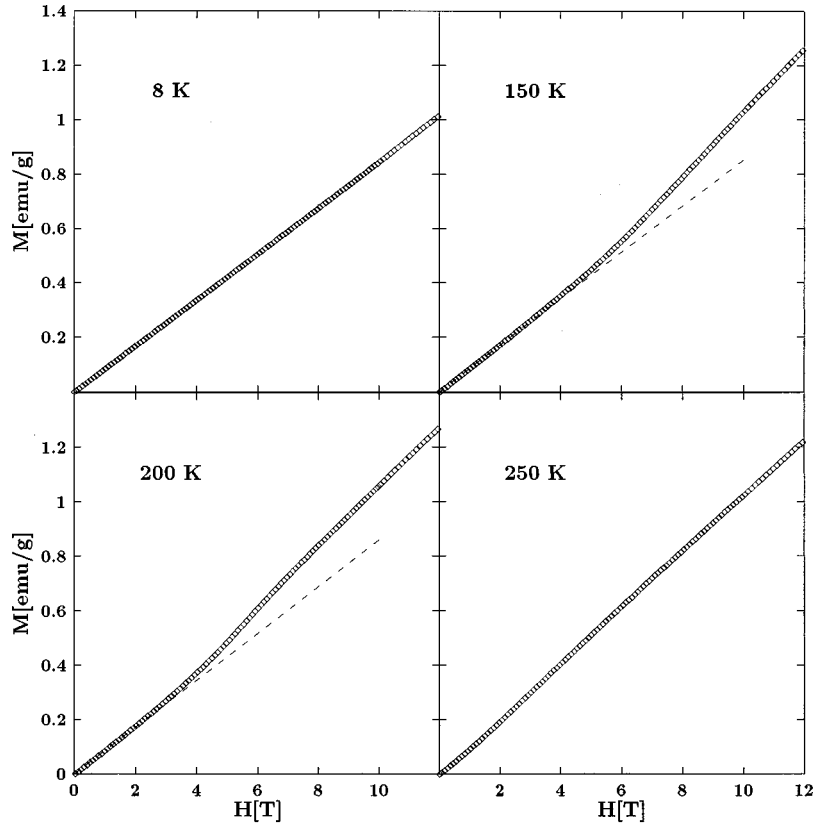


FIG. 4. Magnetization vs magnetic field up to 12 T for YBaCuFeO₅ at 8, 150, 200, and 250 K. The calculated magnetizations according to Eqs. (1) and (2) with the parameters of Table IV agree very well with the observed ones, and the difference is smaller than the size of the symbols. These curves are not shown for clarity, but the extrapolations of the linear behaviors at 150 and 200 K to emphasize the existence of field-induced phase transitions. No significant hystereses have been observed for increasing vs decreasing field strength.

$$+ M_2[1 + \tanh(H - H_C)/\sigma]}, \quad (1)$$

with

$$M_1 = \chi H \quad \text{and} \quad M_2 = \alpha H + M_0. \quad (2)$$

The field-induced transition is broadened thermally as well as due to powder statistics by the dependence of the critical field strength on the specific field orientation in each crystallite. The pronounced deviations from linear behavior at 150 and 200 K are emphasized by the extrapolation of the low-field slope. The best fitting parameters are summarized in Table IV and suggest field-induced transitions at 150 and 200 K from a low-temperature magnetic structure below $T_{N2} \approx 240$ K into the intermediate phase between T_{N1} and T_{N2} in zero field. This phase transition can only take place below T_{N2} and therefore no such transition is observed at 250 K. No field-induced transition is observed at 8 K either, but for a different reason. A critical field strength greater than 12 T is estimated by extrapolation to this low temperature.

The temperature dependence of the molar magnetic susceptibility of (Y_{0.94}Ca_{0.06})CuFeO_{4.95} and the inverse is shown in Fig. 3. The data follow a Curie-Weiss law in the temperature range from 350 to 500 K, with $C = 4.76$ emu K mol⁻¹ and $\theta = -790$ K. These values suggest that strong short-range antiferromagnetic interactions are present in the iron-copper sublattice. A broad peak is observed around $T_{N1} \approx 325$ K; this transition is shifted by about 150 K to lower

temperatures with respect to the value observed for the undoped compound ($T_{N1} \approx 475$ K). The anomaly observed around 100 K can be assigned to the second antiferromagnetic transition found in YBaCuFeO₅ at $T_{N2} \approx 240$ K. As stated above, the calcium doped materials show some degree of oxygen deficiency; the same situation in calcium-doped YBa₂Cu₃O₇ is considered to result from a constant oxidation state for the copper ions.²³ The shift of the ordering temperature to lower values may be a consequence of the oxygen vacancies in the BO₂ layers that break down some B-O-B superexchange paths. Indeed, the magnetic phase transition AF1 → AF2 seems to be suppressed in the calcium-containing compounds, probably due to the weakness of the magnetic superexchange within the BO₂ planes. The magnetic behavior of the LnBaCuFeO_{5±δ} (Ln=lanthanide) compounds seems to be very sensitive to the oxygen content; both the oxygen-deficient (Y_{0.94}Ca_{0.06})BaCuFeO_{4.95} and the oxygen-excess compounds PrBaCuFeO_{5.24} (Refs. 9 and 18) and NdBaCuFeO_{5.18} (Ref. 3) have very different magnetic properties from those of the parent material YBaCuFeO₅.

Refinement of the magnetic structures

The magnetic structures of YBaCuFeO₅ have been deduced from neutron powder-diffraction experiments performed at 600 K ($>T_{N1}$), room temperature (between T_{N1} and T_{N2}), and at 200, 150, and 8 K (all below T_{N2}).

The magnetic unit cell at room temperature consists of four chemical cells, $a_m = \sqrt{2}a$ and $c_m = 2c$. To allow for

TABLE II. Dependence of the magnetic R values on the canting angle in YBaCuFeO_5 at room temperature (left) and 8 K (right).

$\vartheta/^\circ$	R_{mag}	$\vartheta/^\circ$	R_{mag}
0	0.407	0	0.314
46.3	0.289	35.8	0.262
59.1	0.277	49.3	0.241
54.2	0.274	54.7	0.237
50.1	0.278	61.5	0.242
90	0.292	90	0.259

canting of the magnetic moments with respect to the fourfold rotational axis, the magnetic structures are refined in space group $P-1$. The best agreement between calculated and observed intensities is achieved for a collinear model with $\mu = 1.45(5)\mu_B$ and a canting angle $\vartheta = 55(5)^\circ$ to the c axis, the magnetic moments within one chemical cell being antiparallel to each other. The uncertainty in the canting angle has been estimated from its effect on the magnetic R value as given in Table II. This phase will be referred to as AF1. The upper section in Fig. 1 shows the observed data, the pattern calculated using the above model (crystallographic and magnetic structures), and their difference.

In the diffraction patterns recorded at temperatures below T_{N2} , a significant splitting of the magnetic reflections of AF1 is observed, most clearly for the reflection $(\frac{1}{2} \frac{1}{2} \frac{1}{2})$ in AF1 that is split into $(\frac{1}{2} \frac{1}{2} \frac{3}{8})$ and $(\frac{1}{2} \frac{1}{2} \frac{5}{8})$ in the new magnetic phase AF2 (see bottom of Fig. 1). The magnetic unit cell of AF2 is similar to that of AF1 with $a_M = a_m$, but a fourfold increase in c , i.e., $c_M = 4c_m = 8c$. Only reflections with $h_M + k_M$ and l_M odd appear, reducing the number of independent magnetic moments to 8, e.g., those in four successive chemical cells along $[001]$. Only one collinear model gives a good agreement between observed and calculated intensities: again the magnetic moments within one chemical cell are antiparallel, but the sequence along $[001]$ is more complicated than in AF1. A schematic representation of both phases is shown in Fig. 5 for comparison. If the magnetic unit cell of AF1 is denoted as A , then the magnetic unit cell of AF2 is built up from a sequence $AA-A-A$ along $[001]$. The magnetic moments are refined to values of $2.35(15)\mu_B$ at 8 K and $2.15(15)\mu_B$ at 150 K and 200 K, respectively, and the same canting angle $\vartheta = 55(5)^\circ$ as refined for AF1 at room temperature. Table III summarizes the structural parameters for YBaCuFeO_5 at 8 K.

The magnetic phase of YBaCuFeO_5 at low temperatures is formed by a rearrangement of the spins along the $[001]$

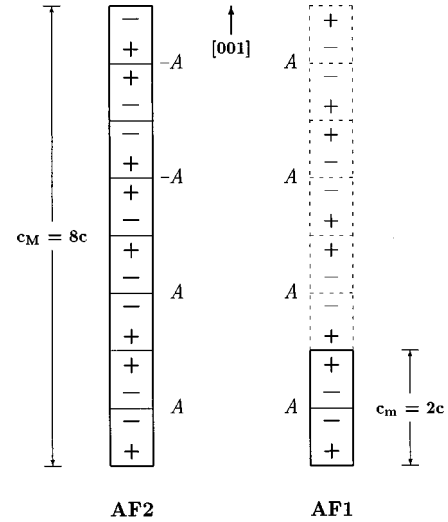


FIG. 5. Schematic representation of the spin sequences along $[001]$ for the two collinear antiferromagnetic phases AF1 and AF2. If the magnetic unit cell of AF1 is denoted as A , the unit cell of AF2 is built up from a sequence $AA-A-A$ along $[001]$.

direction. The transition from AF1 to AF2 with decreasing temperature is accompanied by a flip of half of the spins (A to $-A$). Every four chemical cells, the ferromagnetic ordering across the basal plane of the unit cell, $[+ -][- +]$ or $[- +][+ -]$, changes to an antiferromagnetic ordering, $[- +][- +]$ or $[+ -][+ -]$ as shown in Fig. 5. The latter kinds of spin sequences along the c axis, for which $c_m = c$, have previously been found in $\text{YBaCo}_{2-x}\text{Cu}_x\text{O}_5$ ($0.3 < x < 0.5$),¹⁵ $\text{YBaCoCu}_{0.5}\text{Fe}_{0.5}\text{O}_5$,¹⁷ and more recently in the stoichiometric phase of the praseodymium-containing compound PrBaCuFeO_5 ,¹⁸ all of them isostructural with the title compound YBaCuFeO_5 . Even for the latter, Caignaert *et al.*⁸ have observed in the neutron-diffraction patterns recorded at low temperature some magnetic reflections with indices $(h/2, k/2, l)$ (l integral) corresponding to a magnetic unit cell $a_m = \sqrt{2}a$ and $c_m = c$.

The transformation from AF1 to AF2 can take place via intermediate phases, similar to the *turn angle* phases between AF1 and AF2 in YBCO.¹⁴ The presence of splitting and peak broadening in the diffraction patterns, recorded at 150 and 200 K, may reflect some intermediate state between AF1 and AF2. A magnetic unit cell with c_M of about 60 Å will be very sensitive to stacking faults along $[001]$; thus, the AF1 to AF2 transition can proceed through some unusual sequences along $[001]$, such as incommensurate or long-periodic inter-

TABLE III. Structural parameters for YBaCuFeO_5 at 8 K. S.G: $P4/mmm$, $a = 3.8693(2)$ Å, $c = 7.6389(4)$ Å, $V = 114.4(1)$ Å³, $R_p = 0.075$, $R_{\text{wp}} = 0.101$, $R_{\text{Mag}} = 0.237$, $\chi^2 = 3.6$.

Atom	Site	x/a	y/b	z/c	Occupation	$B_{\text{eq}}/\text{Å}^2$
Ba	1a	0	0	0	1	0.72(9)
Y	1b	0	0	$\frac{1}{2}$	1	0.42(7)
Cu/Fe	2h	$\frac{1}{2}$	$\frac{1}{2}$	0.2684(3)	1/1	0.51(6)
O(1)	4i	$\frac{1}{2}$	0	0.3160(3)	1	0.60(6)
O(2)	1c	$\frac{1}{2}$	$\frac{1}{2}$	0	4	1.1(1)

TABLE IV. Best fitting parameters according to Eqs. (1) and (2) for the field scans $M(H)$ on YBaCuFeO_5 at different temperatures.

T (K)	χ_o [10^{-6} emu/(g G)]	H_c (T)	σ [T]	α [10^{-6} emu/(g G)]	M_0 (10^{-3} emu/g)
8	8.43				
150	8.53	7.1	3.2	10.52	8.0
200	8.59	4.7	2.4	10.52	11.2
250	10.24				

mediate phases. In this connection, Caignaert *et al.*⁸ found an incommensurate phase below T_{N2} with propagation vector $\mathbf{k}=(0,0,0.211)$ at 20 K, referred to the magnetic cell. These authors determined the spin correlation length of about 70 Å by the simultaneous fitting of the magnetic peaks and their satellites. Nevertheless, at sufficient low temperature, the magnetic structure has to lock in commensurately. It is a well-known phenomenon in antiferromagnetic materials exhibiting intermediate phases in zero field, that an external field parallel to the easy direction (which is always the case for some particles in polycrystalline samples) induces (at low temperatures) a transition to the intermediate phase or stabilizes the intermediate phase to lowest temperatures. The pronounced deviations from a linear dependence of magnetization as a function of field in YBaCuFeO_5 at 150 and 200 K, Fig. 4, suggest a field-induced transition, supporting our observation of low (AF2) and intermediate (AF1) temperature magnetic structures.

The partial substitution of yttrium by calcium induces very significant modifications of the magnetic structure of YBaCuFeO_5 . Figure 2 shows the neutron diffraction pattern of $(\text{Y}_{0.94}\text{Ca}_{0.06})\text{BaCuFeO}_{4.95}$ at room temperature. Broad magnetic peaks, associated with short-range interactions within the CuFeO_2 layers, are observed. Well-defined magnetic peaks are also present, the most intense ones have Miller indices $(h/2, k/2, l/2)$, and weak peaks with indices $(h/2, k/2, l)$ are also observed. The latter arise from an antiferromagnetic ordering for which the c axis repeat of the crystallographic unit cell is preserved in the magnetic one. A similar magnetic unit cell has previously been reported for the stoichiometric praseodymium containing material PrBaCuFeO_5 .¹⁸ Even for the parent compound YBaCuFeO_5 , Caignaert *et al.*⁸ have found at low temperature some weak peaks with indices $(h/2, k/2, l)$. As a first attempt, a structure model based on two magnetic phases with propagation vectors $\mathbf{k}_1=(\frac{1}{2}, \frac{1}{2}, \frac{1}{2})$ for phase 1 and $\mathbf{k}_2=(\frac{1}{2}, \frac{1}{2}, 1)$ for phase 2 was refined. The best agreement between calculated and observed intensities is obtained for a collinear model for both phases with the magnetic moments restricted to lie perpendicular to the c axis. The refined magnetic moments are $\mu_1=1.32(5)\mu_B$ and $\mu_2=1.31(18)\mu_B$ for phases 1 and 2, respectively. Due to the low intensity of the peaks corresponding to this second phase, the values of the magnetic moments

are imprecise and the agreement factors are high. The structural and agreement parameters for this model are given in Table I.

The weakness of the magnetic interactions in $(\text{Y}_{0.94}\text{Ca}_{0.06})\text{BaCuFeO}_{4.95}$ prevents the long-range magnetic correlations along [001]. As a consequence, a secondary magnetic phase with unit cell $a_m=\sqrt{2}a$ and $c_m=c$ appears at room temperature, accompanied by a lowering of the order temperature T_{N1} for the predominant phase (AF1). Furthermore, the transition to a low-temperature magnetic phase, observed below T_{N2} in the undoped compound, seems to be hindered. Thus, the magnetic structure of the predominant phase in $(\text{Y}_{0.94}\text{Ca}_{0.06})\text{BaCuFeO}_{4.95}$ in the temperature range from T_{N1} down to 8 K is that determined for YBaCuFeO_5 between T_{N1} and T_{N2} , i.e., AF1.

Neutron-diffraction data, recorded on the calcium-doped sample after thermal treatment in argon atmosphere for 12 h at 873 K, show very broad magnetic peaks and well-defined reflections, revealing a magnetic unit cell $a_m=\sqrt{2}a$ and $c_m=2c$. However, no peaks with indices $(h/2, k/2, l)$ are observed showing that the thermal treatment has modified the magnetic interactions in this material. Thermal treatments in a reducing atmosphere induce in cobalt- and iron-doped $\text{YBa}_2\text{Cu}_3\text{O}_7$ the formation of clusters of the trivalent metal ions.¹³ Also the oxygen content of the calcium-doped material is slightly modified, the actual composition of the sample after the reducing treatment being $(\text{Y}_{0.94}\text{Ca}_{0.06})\text{BaCuFeO}_{4.95(2)}$. Both the clustering of the iron cations and the slight loss of oxygen might account for the change in the magnetic structure of the sample.

ACKNOWLEDGMENTS

The authors thank their colleagues Dr. J. Rodríguez-Carvajal, Dr. J. P. Attfield, and Professor H. Fuess for valuable discussions, and Dr. A. Várez (Universidad Carlos III, Leganés, Madrid) for the TGA measurements. We thank CICYT (Project Mat 95-0809) and MEC (Project HA-141B) for financial support. The neutron-scattering experiments performed at Risø National Laboratory have been supported by the Commission of the European Community (EC) through the Large Installation and the Human Capital and Mobility Programs.

*Author to whom correspondence should be addressed:
Fax: +49 6151 166023; electronic address:
HELMUT@STENO.ST.MW.TU-DARMSTADT.DE

¹L. Er-Rakho, C. Michel, Ph. Lacorre, and B. Raveau, J. Solid State Chem. **73**, 531 (1988).

²C. Meyer, F. Hartman-Boutron, Y. Gros, and P. Strobel, Solid State Commun. **76**, 163 (1990).

³M. Pissas, C. Mitros, G. Kallias, V. Psycharis, A. Simopoulos, A. Kostikas, and D. Niarchos, Physica C **192**, 35 (1992).

⁴M. Pissas, V. Psycharis, C. Mitros, G. Kallias, D. Niarchos, A.

- Koufoudakis, and A. Simopoulos (unpublished).
- ⁵A. W. Mombru, C. Christides, A. Lappas, K. Prasides, M. Pissas, C. Mitros, and D. Niarchos, *Inorg. Chem.* **33**, 1255 (1994).
- ⁶Y. K. Atanassova, V. N. Popov, G. G. Bogachev, N. Ilev, C. Mitros, V. Psycharis, and M. Pissas, *Phys. Rev. B* **47**, 15 201 (1993).
- ⁷J. T. Voughey and K. P. Poeppelmeier, in *Proceedings of the International Conference on Chemistry of Electronic Ceramic Materials*, edited by P. K. Davies and R. S. Roth (U.S. Department of Commerce, NIST Special Publication 804, 1991), p. 419.
- ⁸V. Caignaert, Y. Mirebeau, F. Bourée, N. Nguyen, A. Ducouret, J.-M. Grenèche, and B. Raveau, *J. Solid State Chem.* **114**, 24 (1995).
- ⁹M. J. Ruiz Aragón, U. Amador, E. Moran, and N. H. Andersen, *Physica C* **235-240**, 1609 (1994).
- ¹⁰H. Casalta, P. Schleger, E. Brecht, W. Montfrooij, N. H. Andersen, B. Lebech, W. W. Schmahl, R. Liang, W. N. Hardy, and Th. Wolf, *Phys. Rev. B* **50**, 9688 (1994).
- ¹¹E. Brecht, W. W. Schmahl, H. Fuess, H. Casalta, P. Schleger, B. Lebech, N. H. Andersen, and Th. Wolf, *Phys. Rev. B* **52**, 9601 (1995).
- ¹²P. Zolliker, D. E. Cox, J. M. Tranquada, and G. Shirane, *Phys. Rev. B* **38**, 6575 (1988).
- ¹³I. Mirebeau, E. Suard, V. Caignaert, and F. Bourée, *Phys. Rev. B* **50**, 3230 (1994).
- ¹⁴N. H. Andersen and G. Uimin, *Phys. Rev. B* **56**, 10 840 (1997).
- ¹⁵L. Barbey, N. Nguyen, V. Caignaert, F. Studer, and B. Raveau, *J. Solid State Chem.* **112**, 148 (1994).
- ¹⁶Q. Huang, P. Karen, V. Karen, K. Kjekshus, J. W. Lynn, A. D. Mighell, I. Natisora, N. Rosov, and A. Santoro, *J. Solid State Chem.* **108**, 80 (1994).
- ¹⁷L. Barbey, N. Nguyen, A. Ducouret, V. Caignaert, J. M. Grenèche, and B. Raveau, *J. Solid State Chem.* **115**, 514 (1995).
- ¹⁸M. Pissas, G. Kallias, V. Psycharis, H. Gamari-Seale, D. Niarchos, A. Simopoulos, and R. Sonntag, *Phys. Rev. B* **55**, 397 (1997).
- ¹⁹M. J. Ruiz-Aragón, C. Rial, E. Morán, J. B. Torrance, N. Menéndez, and J. Tornero, *Solid State Ionics* **63-65**, 932 (1993).
- ²⁰J. Rodríguez-Carvajal, *Physica B* **192**, 55 (1993).
- ²¹GSAS 1994. A. C. Larson and R. B. von Dreele, LANSCE, MS-H805, Los Alamos National Laboratory.
- ²²M. J. Ruiz-Aragón, E. Morán, U. Amador, and A. Landa Cánovas (unpublished).
- ²³P. Berastegui, S. G. Eriksson, L. G. Johansson, M. Kakihana, M. Osada, H. Mazaki, and S. Tochihara, *J. Solid State Chem.* **127**, 56 (1996).